

Exchange-Correlation Asymptotics and High Harmonic Spectra

Michael R. Mack^a, Daniel Whitenack^b, Adam Wasserman^{a,b,1}

^a*Department of Chemistry, Purdue University, 560 Oval Drive, West Lafayette, IN 47907, USA*

^b*Department of Physics, Purdue University, 525 Northwestern Ave., West Lafayette, IN 47907, USA*

Abstract

The effect of the asymptotic spatial behavior of the exchange-correlation potential of Time-Dependent Density Functional Theory is investigated for the calculation of high harmonic spectra. We compare the harmonic spectrum of N₂ obtained via the adiabatic local density approximation (A-LDA) and the adiabatic van Leeuwen-Baerends (A-LB94) approximation. Subtle structure in the spectrum is missed by the A-LDA but captured by the A-LB94, a direct consequence of the asymptotic behavior in the *ground-state* exchange-correlation potential. The propagation of the Kohn-Sham orbitals under the two approximations is different and the interference between orbitals, which produces structure in the spectrum, is qualitatively changed.

Keywords: Strong-field Physics; High Harmonic Generation; Time-dependent Density Functional Theory; Adiabatic Local Density Approximation

1. Introduction

High harmonic generation (HHG) in gas phase atoms and molecules is a nonlinear optical process that cannot be theoretically studied using perturbation theory (see Ref. [1–4] for a review). Strong fields distort the electronic

Email addresses: mack3@purdue.edu (Michael R. Mack), dwhitena@purdue.edu (Daniel Whitenack), awasser@purdue.edu (Adam Wasserman)

URL: <http://www.purdue.edu/dft> (Adam Wasserman)

¹Telephone:765-494-2348, Fax:765-494-0239

density creating an oscillating dipole. This oscillation produces bursts of radiation with energy proportional to the fundamental laser frequency as the high energy electrons, which have been accelerated by the field, recombine with the nuclei. The attosecond time scale of these pulses allows one to directly study electron dynamics [5–7].

Theoretically, HHG is commonly described with a semi-classical three-step model: (i) an electron tunnels into the continuum via a distorted coulombic barrier, (ii) it is accelerated by the oscillating field, (iii) and it recollides with the ion resulting in emission of high energy photons [3, 4]. In many cases, interference between orbitals and correlation effects can be ignored. In those instances, the parent atomic or molecular potential through which a single electron tunnels into the continuum is assumed to be untouched by the external field, and the ionized electron is treated as independent of the binding nuclear potential. These approximations are commonly referred to as the strong-field approximation (SFA) within the single active electron approximation (SAEA) [8, 9]. The semi-classical model above has successfully described HHG in atoms, but it fails to account for multielectron contributions to the HHG process in molecules such as N_2 [5, 6, 10–15].

Interference effects which are observed in experimental measurements of HHG in N_2 suggest multiple “active” electrons contribute to the HHG process. A relative phase jump of 0.2π in the harmonic emission of N_2 occurs precisely at a spectral minimum at the 25th harmonic order [12]. One mechanism that connects phase jumps and intensity minima in harmonic spectra was proposed by Lein et al. [16], but this predicted a phase jump of π when a single active electron recollided with the binuclear model system.

Time-dependent density functional theory (TDDFT) [17–19] is an attractive alternative to study HHG because it naturally includes multielectron dynamics by propagating the time-dependent Kohn-Sham (TDKS) equations. In these equations one must approximate the exchange-correlation (XC) potential which is a functional of the electron density at all prior times (memory). Furthermore, the XC potential depends non-locally on the density. The adiabatic local density approximation (A-LDA) which ignores temporal and spatial non-locality is the workhorse of TDDFT. However, we know from ground state DFT that the local density approximation (LDA) suffers from several shortcomings. For example, it fails to support a Rydberg series of bound states and poorly approximates the ionization potential of the system via Koopmans’ theorem [20–22]; these are manifestations of self-interaction error in the LDA [23], and are directly related to the incorrect asymptotic

behavior of the LDA.

We demonstrate here that the structure of HHG spectra is sensitive to the asymptotic behavior of the XC potential, something that has been tacitly assumed in previous works [24–26]. We explicitly display this effect by calculating the HHG spectrum of N₂ with the A-LDA and the A-LB94 [20] approximations, which differ in the asymptotic behavior of their potentials. In the semiclassical picture of HHG, the electrons are pushed far from the nuclei when coupled to an intense electric field, and the Kohn-Sham orbitals of TDDFT are propagated very differently in the asymptotic region using these two potentials. Since the orbitals are used to construct the density and finally the time-dependent dipole moment, subtle differences in orbital interference arise from these different propagations. These subtle differences make themselves visible in the HHG spectrum.

2. High Harmonic Generation and TDDFT

The Runge-Gross theorem establishes a one-to-one correspondence between time-dependent densities and time-dependent potentials for a given initial state [17]. This motivates a set of time-dependent Kohn-Sham (TDKS) equations for N non-interacting particles in a potential $v_s[n](\mathbf{r}, t)$ whose orbitals, $\phi_j(\mathbf{r}, t)$, can be used to construct the time-dependent density, $n(\mathbf{r}, t) = \sum_i^N |\phi_i(\mathbf{r}, t)|^2$, of the N -electron interacting system. The Kohn-Sham orbitals are doubly-occupied in the case of N₂ so we do not specify spin-orbitals. The TDKS equations are solved subject to the constraint that the time-dependent density integrates to the number of electrons of the system. The time-dependent Kohn-Sham potential, $v_s[n](\mathbf{r}, t)$, is a functional of the density and is defined as:

$$v_s[n](\mathbf{r}, t) = v_{\text{ext}}(\mathbf{r}, t) + v_{\text{H}}[n](\mathbf{r}, t) + v_{\text{XC}}[n](\mathbf{r}, t), \quad (1)$$

where

$$v_{\text{H}}[n](\mathbf{r}, t) = \int d\mathbf{r}' \frac{n(\mathbf{r}', t)}{|\mathbf{r} - \mathbf{r}'|} \quad (2)$$

is the Hartree potential and $v_{\text{ext}}(\mathbf{r}, t)$ is the one-body external potential due to not only the electrostatic attraction to the nuclei but also the external electric field. The time-dependent exchange-correlation (XC) potential, $v_{\text{XC}}[n](\mathbf{r}, t)$, accounts for the remaining many-body effects. The exact form of the time-dependent XC potential is unknown but depends on the entire history of the

density (memory) and the initial states of both the interacting and Kohn-Sham systems. We refer to the dependence of $v_{\text{xc}}(\mathbf{r}, t)$ on the density at previous times as *temporal non-locality* and to its dependence on the density at positions other than \mathbf{r} as *spatial non-locality*. For most practical TDDFT calculations, the adiabatic approximation is invoked. This approximation ignores the memory dependence of the XC potential; the potential is approximated as local in time:

$$v_{\text{xc}}^{\text{adia}}[n](\mathbf{r}, t) = v_{\text{xc}}^{\text{GS}}[n(t)](\mathbf{r}), \quad (3)$$

where $v_{\text{xc}}^{\text{GS}}[n(t)]$ is the ground-state XC potential evaluated at the instantaneous density. This approximation is valid for slowly varying potentials, and it is important to understand its limitations in the strong-field regime [27].

In addition to approximating the XC potential as local in time one often approximates $v_{\text{xc}}[n(t)](\mathbf{r})$ by using an adiabatic extension of a ground-state approximation to the XC functional: $v_{\text{xc}}^{\text{adia}}[n](\mathbf{r}, t) \approx v_{\text{xc}}^{\text{approx}}[n(t)](\mathbf{r})$. In this Letter, we explore the capabilities of the computationally advantageous ALDA to the time-dependent XC potential in which artificial dynamics could be induced by both the local approximation in time and space. We then consider the A-LB94 which decays coulombically as the *exact* KS potential does [28].

Consider the locality in time or lack of memory effects (adiabatic approximation). A time-dependent XC potential that ignores memory, or one that is local in time, has been shown to completely fail at even qualitatively describing important phenomena including Rabi oscillations [29]. However, a recent study of a model system by Thiele et al. [30] revealed that the inclusion of memory in the XC potential does not significantly change certain properties such as ionization yields, and we expect memory effects to be small in the calculation of HHG spectra due to the relatively small frequencies typically used. Baer et al. [31] included memory effects in a TDDFT calculation of HHG in gold metal clusters and found the non-adiabatic effects in the XC potential to reduce harmonic intensities, concentrate the spectral peaks near the harmonic order, and decrease the spectral linewidths. In this work we focus on the consequences of approximating the XC functional with the LDA, but a study of memory effects, if they are present, would be valuable.

We take a close look at the nonlocality in space. It is well known that the local density approximation (LDA) incorrectly approximates the asymptotic behavior of the exact XC potential [20]. The LDA potential is directly related to a localized density and therefore decreases exponentially as $r \rightarrow \infty$,

instead of displaying the correct $-1/r$ behavior. The van Leeuwen-Baerends (LB94) approximation explicitly incorporates Coulomb asymptotics to the LDA [20]. The A-LB94 potential (spin-unpolarized) has the form:

$$v_{\text{xc}}^{\text{A-LB94}}[n](\mathbf{r}, t) = v_{\text{xc}}^{\text{A-LDA}}[n](\mathbf{r}, t) - \frac{\beta n^{1/3}(\mathbf{r}, t) s^2(\mathbf{r}, t)}{1 + 3\beta s(\mathbf{r}, t) \sinh^{-1}(s(\mathbf{r}, t))}, \quad (4)$$

where $s(\mathbf{r}, t) = |\nabla n(\mathbf{r}, t)|/n(\mathbf{r}, t)^{4/3}$ and $\beta = 0.05$ is an empirical parameter. The differences between the A-LDA and A-LB94 approximations for N_2 are illustrated in Figure 1 which shows a slice of both approximations along the bond axis at $t = 0$ when the molecule is in its ground-state. The LDA potential approaches zero exponentially and the LB94 potential decays much slower and tends to $-1/r$. It is not surprising that spatial differences far from the nuclei could have some noticeable influence on the harmonic spectrum.

We used the `octopus` [32] code to propagate the time-dependent Kohn-Sham orbitals and study HHG of an aligned nitrogen molecule when exposed to a strong electric field. Interaction with the electric field is treated in the dipole approximation and the length gauge [33]. The code solves the time-dependent Kohn-Sham equations using a uniform, real space grid in real time. Grid spacing in all directions is 0.150 \AA and the simulation is performed in a sphere with a radius of 10 \AA to minimize charge density from escaping the simulation region. The molecular potential is replaced with norm-conserving Troullier-Martins pseudopotentials [34]. The nuclei are positioned parallel to the x-axis with a frozen equilibrium bond length of 1.096 \AA [35]. The strong field interaction is modeled by an oscillating electric field with a sinusoidal envelope polarized along the molecular axis:

$$E(t) = -E_0 \sin\left(\frac{\pi t}{T}\right) \sin(\omega t), \quad (5)$$

where the frequency of the laser $\omega = 1.55 \text{ eV}$ and the peak intensity $I_0 = 2 \times 10^{14} \text{ W/cm}^2$, typical in strong field experiments with N_2 [5, 6, 10–15]. Memory effects should be negligible for this range of ω which can be motivated by a previous study [30]. The case of N_2 is interesting because the energy difference between the two most important ionization channels is close to this frequency [36]. Peak intensity occurs at half the laser pulse which is terminated after $T = 36 \text{ fs}$ (13 optical cycles). The Kohn-Sham orbitals were propagated using an approximate time-reversal symmetry scheme with a time step of $\Delta t = 6.6 \times 10^{-19} \text{ s}$ [37]. At this intensity, some charge density is

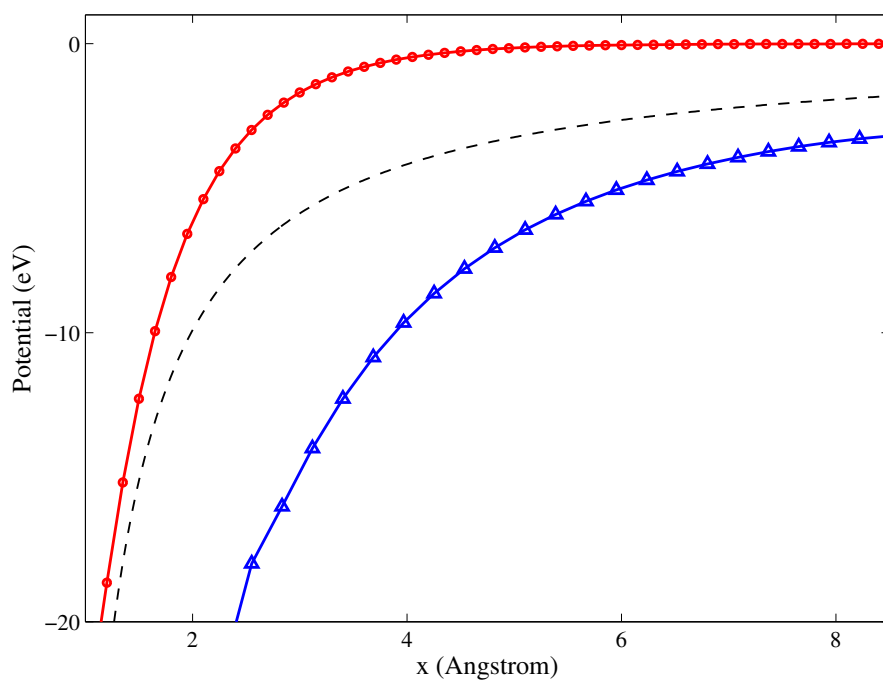


Figure 1: Comparison of the ground-state XC potentials for N_2 and exact ground state XC decay along the bond axis: v_{xc}^{A-LDA} (circle), v_{xc}^{A-LB94} (triangle), Coulomb decay (dashed line).

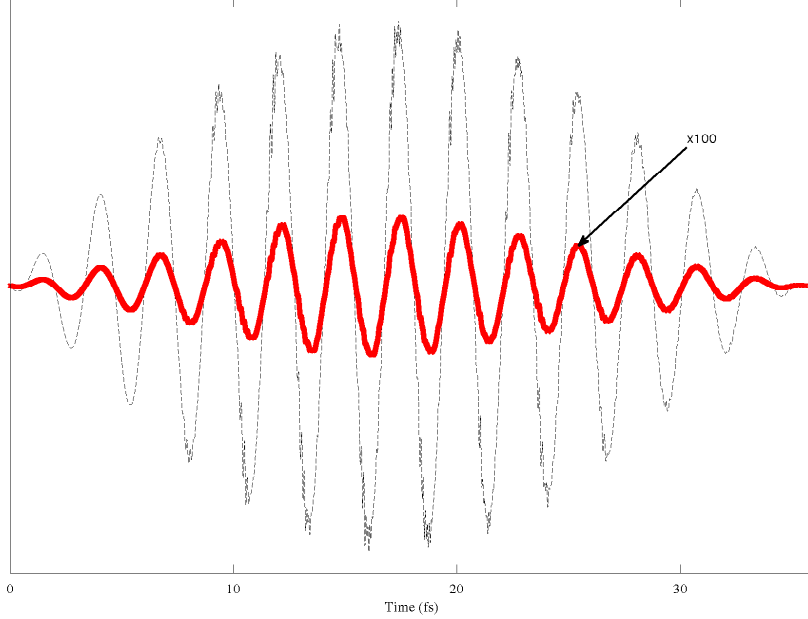


Figure 2: Time-dependent dipole and dipole acceleration of N_2 in the direction of laser polarization. (solid) A-LDA dipole moment (y-axis: $e\text{\AA}$). (dashed) A-LDA acceleration dipole (y-axis: $e\text{\AA}(eV/\hbar)^2$). Note: $\hbar = 6.582 \times 10^{-16} \text{ eV} \cdot \text{s}$.

expected to be so far removed from the nuclei that it will never return. This ionization is accounted for using a masking function which does not affect the orbitals inside the simulation region, but gradually forces the orbitals to zero at the boundaries.

Calculating the harmonic spectrum of N_2 along the polarization axis requires knowledge of the time-dependent dipole at each time step. The induced dipole along the polarization axis at time t is calculated by the integral:

$$d(t) = \int d\mathbf{r} \ x n(\mathbf{r}, t). \quad (6)$$

Figure 2 shows the calculated dipole moment and dipole acceleration from the propagation with the A-LDA. The harmonic spectrum in the direction of polarization is calculated by taking the Fourier transform of the dipole

acceleration:

$$H(\omega) = \left| \int dt e^{i\omega t} \frac{d^2}{dt^2} d(t) \right|^2. \quad (7)$$

The acceleration $a(t)$ dipole in the direction of polarization is calculated using the Ehrenfest Theorem [38]:

$$a(t) = \frac{d^2}{dt^2} d(t) = - \int d\mathbf{r} n(\mathbf{r}, t) \nabla v_s(\mathbf{r}, t). \quad (8)$$

We compare calculated harmonic spectra using the A-LDA and A-LB94 approximations for the XC potential. In both cases we neglect non-locality in time via the adiabatic approximation.

3. Results and Discussion

Using the electric field parameters described above, the harmonic spectrum of N_2 predicted by TDDFT within the A-LDA is presented in Figure 3. The molecular axis was fixed along the polarization direction of the electric field. Well defined odd-order harmonics are predicted for N_2 up to order 35 (54 eV). The harmonic radiation intensity peaks at the 23rd harmonic order and is followed by successively smaller peaks until about the 35th order. High intensity yields are observed for orders 15 through 29, whereas the lower harmonic orders (except for the fundamental) are almost completely absent. This lack of intensity in the low harmonic orders is due to the destructive interference of Kohn-Sham orbitals. We have verified this by freezing all Kohn-Sham orbitals except the highest occupied orbital (KS-HOMO) in the propagation (a type of SAEA). In this calculation, the intensity of the low harmonic orders increases and is comparable with the higher-order intensities.

To demonstrate any dependence on the asymptotic behavior of the XC potential, we calculated the harmonic spectrum of N_2 using the A-LB94 XC potential (with the same external field parameters). This spectrum is presented in Figure 4. The A-LB94 calculation predicts harmonics at exactly the same orders as the A-LDA spectrum; however, this approximation yields a slightly different structure in the harmonic orders 21 - 25. Interestingly, the A-LB94 calculation shows an intensity minimum located at the 25th harmonic order, similar to the minimum observed experimentally [5, 6, 10, 12, 15] that is not present in the A-LDA calculation. Although it seems that there could

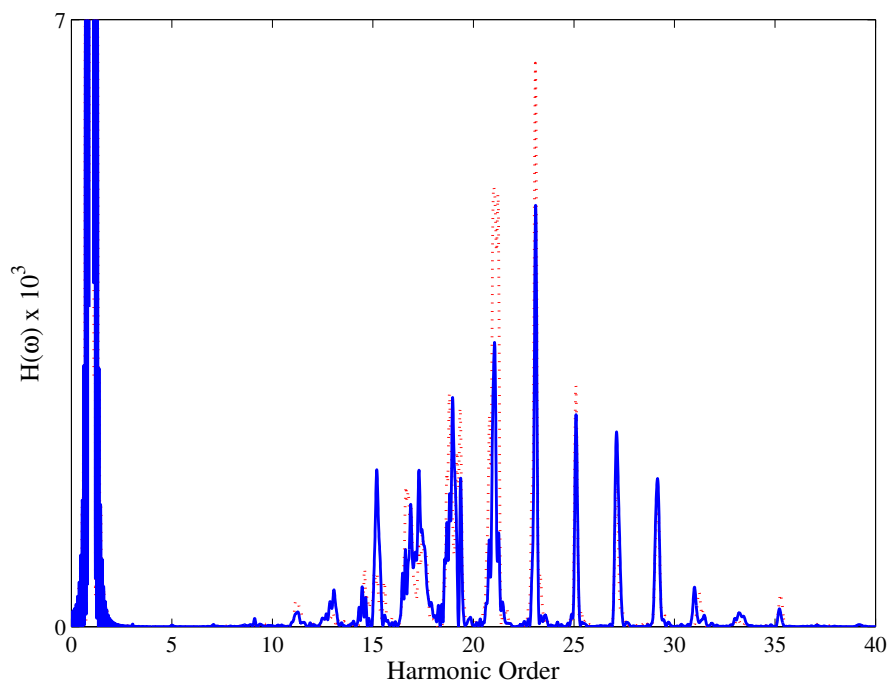


Figure 3: Harmonic spectrum of N₂ within the A-LDA with on (dotted) and off (solid) resonant laser frequencies (see text for values).

be some subtle structure around the 25th harmonic in the A-LDA spectrum, the A-LB94 spectrum has a well-defined minimum resulting purely from the behavior of the XC potential far from the nuclei. In addition, the most intense harmonic is shifted from the 23rd harmonic in the A-LDA calculation to the 21st harmonic in the A-LB94 calculation. Also the entire span of peaks in the A-LB94 calculation have only a fraction of the intensity as those in the A-LDA calculation.

We consider a semiclassical explanation for why the correct asymptotic behavior of the XC potential is important in HHG calculations. The KS orbitals are dragged far from the initial ground state by the intense electric field. The electrons then recombine with the other orbitals after being accelerated back toward the nuclei, and have the possibility of interfering with each other. In such a recombination, the rate at which the potential decays directly influences the phase shift of the recombining orbital. Therefore, two identical systems differing only in the asymptotic behavior of their respective potentials and propagated in the same external field (which pushes the orbitals far from equilibrium) will likely display different interference effects. In the case of N₂, the different asymptotes of the A-LDA and A-LB94 XC potentials yield different interference effects at the 25th harmonic order. Interference in the Kohn-Sham orbitals would also increase the relative intensity of the 21st harmonic relative to the 23rd in the case of the A-LB94 calculation.

Yet, it might not be fair to compare the spectrum of an A-LDA and A-LB94 calculation at the same frequency of $\omega = 1.55$ eV because the actual energy difference between the Kohn-Sham (KS) HOMO and KS HOMO-1 in the two approximations is different. In either case the KS orbitals are close in energy and the electron dynamics could be more sensitive to a resonant frequency in the applied field. In other words, one might not expect the A-LDA spectrum at this frequency to have strong mixing between these two highest energy orbitals because the frequency is not resonant with the approximate excitation in the theory. To explore this question, we did the same calculation at a laser frequency of $\omega = 1.51$ eV, which corresponds to the LDA HOMO-1 \rightarrow LDA HOMO transition energy. The new spectrum at this frequency is also presented in Figure 3. One can see that the structure of this spectrum has not changed significantly. The minimum at the 25th harmonic, which is present in the A-LB94 calculation, is still absent from the A-LDA spectrum. This indicates that some of the important structure in the harmonic spectrum of N₂ can only be captured by an approximation

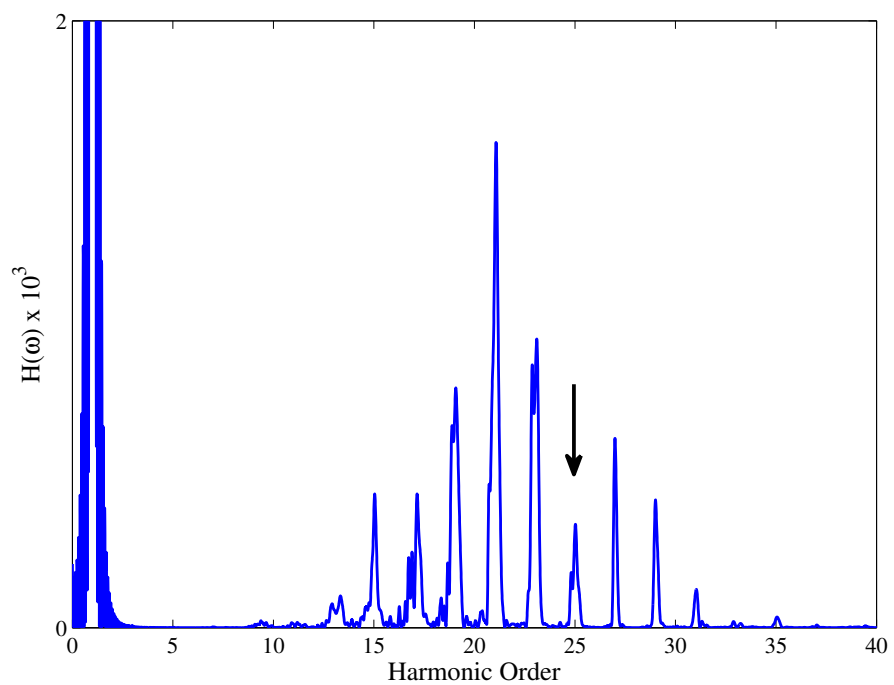


Figure 4: Harmonic spectrum of N₂ using the A-LB94 XC potential. The arrow points to an intensity minimum absent from the A-LDA calculation, but observed experimentally (see text for citations).

that includes Coulomb XC asymptotics. Similar features likely exist in the HHG spectrum of other systems when multielectron effects are not negligible.

Although differences arising from XC asymptotics can be seen by examining the resulting spectra, we can also understand such behavior by looking at the propagation of the TDKS equations. The KS orbitals are propagated in time via a time-propagation operator, $\hat{U}_s = \exp(i\hat{H}_s t)$, where \hat{H}_s is the KS Hamiltonian. At large r , A-LDA and A-LB94 produce propagators with markedly different behavior. Using an exponential decay, $-Ce^{-Br}$ (C and B are constants), of the LDA XC potential and the $-1/r$ decay of the LB94 XC potential, Taylor expanding the exponential time propagator, and ignoring like terms gives:

$$\hat{U}_s^{LDA} = \hat{1} - iCe^{-Br} - \frac{C^2 e^{-2Br}}{2} + \frac{BCe^{-Br}}{4} + \dots, \quad (9)$$

$$\hat{U}_s^{LB94} = \hat{1} - i\frac{B}{r} - \frac{B}{2r} - \frac{B}{4r^2} + \dots, \quad (10)$$

as $r \rightarrow \infty$. Then taking the leading terms we see that:

$$\hat{U}_s^{LDA} = \hat{1} + (\text{constant})r + O(r^2) \quad (11)$$

$$\hat{U}_s^{LB94} = \hat{1} + (\text{constant})\frac{1}{r} + O\left(\frac{1}{r^2}\right) \quad (12)$$

Therefore, an A-LDA approximation to the time-propagation tends to over-propagate the asymptotic regions compared with the $-1/r$ decay. This strong propagation of the orbitals in the asymptotic regions drowns out subtle features such as the minimum seen in the A-LB94 spectrum of N_2 and observed experimentally [5, 6, 10, 15].

4. Conclusion

With the wealth of evidence that multielectron effects are responsible for the intensity minimum in the N_2 harmonic spectrum, TDDFT is useful for predicting such characteristics since it is an all-electron theory. However one must take careful note of subtle structure that might be missed by spatially local approximations.

We have shown that the A-LDA misses structure in the spectrum due to interference effects. The LB94 potential, which decays as $-1/r$, produces a clear intensity minimum at the 25th harmonic order. Thus, inaccuracies

in the harmonic spectrum of N_2 calculated with approximate TDDFT are not necessarily a consequence of the adiabatic approximation but could be a manifestation of the failure of the approximate ground-state functional to satisfy important exact conditions.

Understanding the exact dynamics of the Kohn-Sham system including spatial and temporal nonlocality is a formidable task. However, HHG is an excellent test case to study some of the consequences of widely used approximations. How avoiding *temporal nonlocality* influences HHG spectra, will be addressed in future work.

5. Acknowledgments

We acknowledge valuable discussions with Neepa Maitra and Roi Baer. This work was supported by the Purdue Research Foundation, the Donors of the American Chemical Society Petroleum Research Fund grant No.PRF# 49599-DNI6 and the National Science Foundation CAREER program grant No. CHE-1149968. We also acknowledge computational time provided on the Odyssey cluster supported by FAS research computing group at Harvard University.

References

- [1] A. L’Huillier, K. J. Schafer, K. C. Kulander, Theoretical aspects of intense field harmonic generation, *Journal of Physics B: Atomic, Molecular and Optical Physics* 24 (1991) 3315–3341.
- [2] J. L. Krause, K. J. Schafer, K. C. Kulander, Calculation of photoemission from atoms subject to intense laser fields, *Phys. Rev. A* 45 (1992) 4998–5010.
- [3] P. B. Corkum, Plasma perspective on strong field multiphoton ionization, *Physical Review Letters* 71 (1993) 1994–1997.
- [4] M. Lewenstein, P. Balcou, M. Y. Ivanov, A. L’Huillier, P. B. Corkum, Theory of high-harmonic generation by low-frequency laser fields, *Physical Review A* 49 (1994) 2117–2132.
- [5] J. Itatani, J. Levesque, D. Zeidler, H. Niikura, H. Pepin, J. C. Kieffer, P. B. Corkum, D. M. Villeneuve, Tomographic imaging of molecular orbitals, *Nature* 432 (2004) 867–871.

- [6] B. K. McFarland, J. P. Farrell, P. H. Bucksbaum, M. Gühr, High Harmonic Generation from Multiple Orbitals in N₂, *Science* 322 (2008) 1232–1235.
- [7] O. Smirnova, Y. Mairesse, S. Patchkovskii, N. Dudovich, D. Villeneuve, P. Corkum, M. Y. Ivanov, High harmonic interferometry of multi-electron dynamics in molecules, *Nature* 460 (2009) 972–977.
- [8] O. Smirnova, M. Spanner, M. Ivanov, Analytical solutions for strong field-driven atomic and molecular one- and two-electron continua and applications to strong-field problems, *Physical Review A* 77 (2008) 033407.
- [9] W. Li, X. Zhou, R. Lock, S. Patchkovskii, A. Stolow, H. C. Kapteyn, M. M. Murnane, Time-Resolved Dynamics in N₂O₄ Probed Using High Harmonic Generation, *Science* 322 (2008) 1207–1211.
- [10] B. K. McFarland, J. P. Farrell, P. H. Bucksbaum, M. Gühr, High-order harmonic phase in molecular nitrogen, *Phys. Rev. A* 80 (2009) 033412.
- [11] R. M. Lock, X. Zhou, W. Li, M. M. Murnane, H. C. Kapteyn, Measuring the intensity and phase of high-order harmonic emission from aligned molecules, *Chemical Physics* 366 (2009) 22–32.
- [12] J. Farrell, B. McFarland, M. Gühr, P. Bucksbaum, Relation of high harmonic spectra to electronic structure in N₂, *Chemical Physics* 366 (2009) 15 – 21.
- [13] X. Zhou, R. Lock, N. Wagner, W. Li, H. C. Kapteyn, M. M. Murnane, Elliptically Polarized High-Order Harmonic Emission from Molecules in Linearly Polarized Laser Fields, *Physical Review Letters* 102 (2009) 073902.
- [14] C. F. de Morisson Faria, X. Liu, Electron–electron correlation in strong laser fields, *Journal of Modern Optics* 58 (2011) 1076–1131.
- [15] Mairesse, Y., Levesque, J., Dudovich, N., Corkum, P. B., Villeneuve, D. M., High harmonic generation from aligned molecules-amplitude and polarization, *Journal of Modern Optics* 55 (2008) 2591–2602.

- [16] M. Lein, N. Hay, R. Velotta, J. P. Marangos, P. L. Knight, Role of the Intramolecular Phase in High-Harmonic Generation, *Phys. Rev. Lett.* 88 (2002) 183903.
- [17] E. Runge, E. K. U. Gross, Density-Functional Theory for Time-Dependent Systems, *Phys. Rev. Lett.* 52 (1984) 997–1000.
- [18] M. A. L. Marques, N. T. Maitra, F. M. S. Nogueira, E. K. U. Gross, A. Rubio (Eds.), *Fundamentals of Time-Dependent Density Functional Theory*, vol. 837 of *Lecture Notes in Physics*, Springer, 2012.
- [19] C. A. Ullrich, *Time-Dependent Density-Functional Theory: Concepts and Applications (Oxford Graduate Texts)*, Oxford University Press, USA, 2012.
- [20] R. van Leeuwen, E. J. Baerends, Exchange-correlation potential with correct asymptotic behavior, *Phys. Rev. A* 49 (1994) 2421–2431.
- [21] J. P. Perdew, M. Levy, Comment on “Significance of the highest occupied Kohn-Sham eigenvalue”, *Phys. Rev. B* 56 (1997) 16021–16028.
- [22] A. Wasserman, N. T. Maitra, K. Burke, Accurate Rydberg Excitations from the Local Density Approximation, *Phys. Rev. Lett.* 91 (2003) 263001.
- [23] J. P. Perdew, A. Zunger, Self-interaction correction to density-functional approximations for many-electron systems, *Physical Review B* 23 (1981) 5048–5079.
- [24] E. P. Fowe, A. D. Bandrauk, Nonlinear time-dependent density-functional-theory study of ionization and harmonic generation in CO₂ by ultrashort intense laser pulses: Orientational effects, *Physical Review A* 81 (2010) 023411.
- [25] J. Heslar, D. Telnov, S. I. Chu, High-order-harmonic generation in homonuclear and heteronuclear diatomic molecules: Exploration of multiple orbital contributions, *Physical Review A* 83 (2011) 043414.
- [26] E. Penka Fowe, A. D. Bandrauk, *Phys. Rev. A* 84 (2011) 035402.

- [27] M. Marques, C. Ullrich, F. Nogueira, A. Rubio, K. Burke, E. Gross (Eds.), *Time-Dependent Density Functional Theory*, Lecture Notes in Physics, Springer, 2006, 1–13.
- [28] C. O. Almbladh, U. von Barth, Exact results for the charge and spin densities, exchange-correlation potentials, and density-functional eigenvalues, *Physical Review B* 31 (1985) 3231–3244.
- [29] J. I. Fuks, N. Helbig, I. V. Tokatly, A. Rubio, Nonlinear phenomena in time-dependent density-functional theory: What Rabi oscillations can teach us, *Phys. Rev. B* 84 (2011) 075107.
- [30] M. Thiele, E. K. U. Gross, S. Kümmel, Adiabatic Approximation in Non-perturbative Time-Dependent Density-Functional Theory, *Phys. Rev. Lett.* 100 (2008) 153004.
- [31] Y. Kurzweil, R. Baer, Quantum memory effects in the dynamics of electrons in gold clusters, *Phys. Rev. B* 73 (2006) 075413.
- [32] A. Castro, H. Appel, M. Oliveira, C. A. Rozzi, X. Andrade, F. Lorenzen, M. A. L. Marques, E. K. U. Gross, A. Rubio, octopus: a tool for the application of time-dependent density functional theory, *phys. stat. sol. (b)* 243 (2006) 2465–2488.
- [33] E. Cormier, P. Lambropoulos, Optimal gauge and gauge invariance in non-perturbative time-dependent calculation of above-threshold ionization, *Journal of Physics B: Atomic, Molecular and Optical Physics* 29 (1996) 1667–1680.
- [34] N. Troullier, J. L. Martins, Efficient pseudopotentials for plane-wave calculations, *Physical Review B* 43 (1991) 1993–2006.
- [35] D. R. Lide, *CRC Handbook of Chemistry and Physics*, 88th Edition, CRC, 2007.
- [36] Y. Mairesse, J. Higuët, N. Dudovich, D. Shafir, B. Fabre, E. Mével, E. Constant, S. Patchkovskii, Z. Walters, Yu, O. Smirnova, High Harmonic Spectroscopy of Multichannel Dynamics in Strong-Field Ionization, *Physical Review Letters* 104 (2010) 213601.

- [37] M. Marques, C. Ullrich, F. Nogueira, A. Rubio, K. Burke, E. Gross (Eds.), Time-Dependent Density Functional Theory, Lecture Notes in Physics, Springer, 2006, 197–210.
- [38] C. Fiolhais, F. Nogueira, M. Marques (Eds.), A Primer in Density Functional Theory, Lecture Notes in Physics, Springer, 2003, 144–184.